Int J Clin Exp Pathol 2017;10(11):10792-10801
www.ijcep.com /ISSN:1936-2625/IJCEP0064043

Original Article

Recombined human endostatin (Endostar) enhances cisplatin delivery and potentiates chemotherapy by decompressing colorectal cancer vessels

Xiaoxu Zhao[1*], Jinghua Pan[1*], Yan Song[2], Hui Ding[1], Li Qin[3], Yunlong Pan[1]

[1]Department of General Surgery, The First Affiliated Hospital of Jinan University, Guangzhou, China; [2]Department of Pathology, The First Affiliated Hospital of Sun Yat-sen University, Guangzhou, China; [3]Department of Histology and Embryology, Medical School of Jinan University, Guangzhou, China. [*]Equal contributors.

Received August 20, 2017; Accepted October 17, 2017; Epub November 1, 2017; Published November 15, 2017

Abstract: Tumor vessels are continuously compressed by solid stress from tumor interstitial matrix, contributing to limited vessel perfusion and oxygen delivery, in which, Collagen plays an important role in transmitting the solid stress to tumor vessels. Therefore, it is urgent to explore novel drugs targeting solid stress, which can increase vessel perfusion as well as drug delivery in cancers. We demonstrate that recombined human endostatin (Endostar) could decrease colorectal cancer associated fibroblasts (CAF) density, reduces tumor stromal collagen I production, and decrease the expression of profibrotic signals, including vascular endothelial growth factor (VEGF), connective tissue growth factor (CTGF) as well as transforming growth factor β1 (TGF-β1). Consequently, Endostar was able to relieve solid stress in tumor, leading to increased vessel perfusion. Following this mechanism, oxygen as well as cisplatin delivery were promoted by Endostar, leading to alleviated hypoxia and chemotherapy sensitivity in colorectal cancer model. Taken together, Endostar could be utilized as a potential agent to effectively decompress tumor vessels and to inhibit tumor growth through its therapeutic function.

Keywords: Recombined human endostatin, colorectal cancer, vessel decompression, solid stress, connective tissue growth factor, cancer associated fibroblasts

Introduction

The organization as well as delivery efficien-cy of perfused vessels largely determine the oxygen and drug delivery in tumor tissues [1, 2]. But the tumor vessels are abnormally compressed because of solid stress within the tumor microenvironment, gradually leading to hypoxia in tumor [3]. With the proliferation of both cancer cells and stromal cells in tumor microenvironment, the accumulation of solid stress progresses due to the crosstalk of multiple matrix molecules [4]. The storage of the stress by the matrix gradually transimits throughout the tumor to collapse vessels, subsequently leading to inhomogeneous and poor perfusion and hypoxia in the tumor. Together, these factors facilitate tumor progression [5, 6]. Previous studies have observed less sensitive chemotherapy response as well as shorter survival in patients with low tumor perfusion compared to those with high perfusion [7, 8]. Therefore, it is urgent to explore novel drugs targeting solid stress, which can increase vessel perfusion as well as drug delivery in cancers.

The tumor mass consists of a considerable number of cancer associated fibroblasts (CAF), which is able to produce and maintain the extracellular matrix (ECM). The excessive proliferation of these stromal cells triggers desmoplastic responses, characterized by the accumulation of hyaluronan, collagen fibers as well as other ECM molecules [9, 10]. Despite the well-known contribution of CAF and matrix to solid stress, the precise mechanisms of the complex interactions among these factors to compress vessels is unidentified. Therefore, elucidating the mechanisms of tumor vessels compression would complement the paradigms for increasing tumor perfusion.

Angiogenesis is recognized to be a core factor in tumor growth as well as metastasis and anti-

angiogenesis therapy has complemented the cancer regimens [11]. Endostatin is the strongest endogenous angiogenesis inhibitor, which inhibits vascular endothelial growth factor (VEGF) expression and then inhibits tumor angiogenesis [12]. Endostar, a modified recombinant human endostatin, presents with a more steady structure due to the added nine-amino acid sequence at the N-terminus, and maintains its original biological function [13]. A recent study has demonstrated that a higher clinical benefit response (CBR) as well as longer progression-free survival (PFS), along with tolerate adverse events, were observed in advanced soft tissue sarcoma after a combined treatment of Endostar and chemotherapy [14].

Endostar has been previously classified as antiangiogenics, however, here, Endostar was shown to decrease colorectal cancer xenografts CAF density, to reduce the production of collagen I, and to decrease expression of profibrotic signals, including TGF-β1, CTGF as well as VEGF. Moreover, Endostar was able to reduce solid stress and subsequently to decompress colorectal cancer vessels, which enhanced both oxygen and cisplatin delivery, finally leading to improved chemotherapy effects. Therefore, targeting solid stress could lead to enhanced tumor perfusion as well as better chemotherapy outcomes via expression decline in matrix collagen as well as other agents in tumor tissues.

Materials and methods

Reagents and cells

Endostar was provided by Simcere-Medgenn Bio-pharmaceutical Co., Ltd (Shandong, China) and stored at 4°C. Cisplatin was purchased from Jiangsu Hao Sen Pharmaceutical Co., Ltd (Jiangsu, China). The colorectal cancer cell line (sw620) was purchased from Type Culture Collection of the Chinese Academy of Sciences (Shanghai, China), cultured in Dulbecco's Modified Eagle's Medium (DMEM) containing 10% fetal bovine serum (Thermo Fisher Scientific, Waltham, MA, USA) and maintained in a 37°C incubator with 5% CO_2.

Colorectal cancer xenograft models and treatment regimens

6-8-week-old female Balb/c nude mice were purchased from the Beijing HFK Bioscience Co., LTD (Beijing, China) and maintained under specific pathogen-free conditions. All animal procedures approved by and conducted in accordance with the guidelines of the Laboratory Animal Ethics Committee of Jinan University. Xenografted colorectal cancer was initiated by injection of 5×10^6 sw620 cells into the subcutaneous tissue of the right flank. The tumor volume was measured using a calliper and calculated as volume = (length × width^2) × 0.523. When the tumor volume reached 100 mm^3 post-inoculation, the mice were divided into two groups (6 mice per group) and treated with 25.0 mg·kg^{-1} Endostar or an equal volume of saline intravenously every other day for 14 days. The blood samples and the tumors were collected and examined on day 14.

Detection of plasma profibrotic signals. Xenograft nude mice blood samples were collected in test tubes and immediately centrifuged at 3500 rpm for 15 min to obtain the plasma samples and stored at -80°C before detection. Levels of TGF-β1, CTGF or VEGF in plasma were measured using ELISA Kit (Phoenix Pharmaceuticals, Burlingame, CA, USA) according to the manufacturer's instructions.

Detection of colorectal cancer profibrotic signals

Tumor tissues were collected and fixed with 4% paraformaldehyde, embedded in paraffin and 4 μm sections were made. The slides were deparaffinized through a series of solutions (100% xylene through 100% ethanol to 100% water) and the prepared slides incubated with alpha-smooth muscle actin (α-SMA) (CAF) (1:200 dilution, Proteintech, Wuhan, China), active TGF-β1 (1:500 dilution, Abcam, Cambridge, UK), CTGF (1:500 dilution, Abcam, Cambridge, UK) or VEGF (1:500 dilution, Abcam, Cambridge, UK) overnight at 4°C, then incubated with goat anti-rabbit IgG (H+L) horseradish peroxidase (1:100 dilution, Beyotime, Jiangsu, China) for 40 min at 37°C. The antibody stainings were visualized with 3,3'-diaminobenzidine (DAB) using fluorescence microscope (Leica DM6000B).

Colorectal cancer stromal collagen I level. For tumor stromal collagen I staining, the tumors were excised, frozen in optimal cutting temperature compound (OCT, Sakura Finetek, Torrance, CA, USA) and stored at -80°C. Cryosections with a thickness of 5 μm were fixed in cold acetone and rehydrated in PBS. Collagen I was

stained with anti-collagen I antibody (1:200, Abcam, Cambridge, UK) overnight at 4°C, and then incubated with FITC-conjugated Affinipure Goat Anti-Rabbit IgG (1:200, Proteintech, Wuhan, China) for 1 h in the dark. The antibody stains were visualized using fluorescence microscope.

Colorectal cancer vascular perfusion

For tumor vascular perfusion studies, nude mice were slowly (~2 min) injected with 10 $mg \cdot kg^{-1}$ FITC-lectin (Sigma-Aldrich, St Louis, MO, USA) on the day of the last treatment, administered via the intravenous injection 10 min before the removal of the tumors. The tumors were then excised, frozen in OCT compound and stored at -80°C. Cryosections with a thickness of 5 μm were fixed in cold acetone and rehydrated in PBS. Then the sections were stained with anti-CD31 antibody (1:500, Abcam, Cambridge, UK), and following incubated with rhodamine goat anti-rat antibody (Proteintech, Wuhan, China; 1:200) for 1 h in the dark. Tissue was visualized under fluorescence microscope, and the percentage of tumor vascular perfusion was calculated as the ratio of the lectin + area to CD31+ area using Image J software.

Detection of colorectal cancer hypoxia

For tumor hypoxia studies, the nude mice were intraperitoneally injected with 60 $mg \cdot kg^{-1}$ of pimonidazole 1 h before the removal of tumors. Then the tumors were fixed and sections were made as described above. Hypoxyprobe-1 Plus kit (HPI Inc, Burlington, MA, USA) was used for pimonidazole staining according to the manufacturer's instructions. Hypoxyprobe-1 adducts were examined with an affinity-purified rabbit IgG polyclonal antibody conjugated with horseradish peroxidase (1:100, Beyotime, Haimen, China).

Histological image analysis

Six random fields at × 200 magnification were taken from each slide using fluorescence microscope. For vascular perfusion fraction, the number of vessels counted by this program with colocalization of lectin and CD31 staining was divided by the number of vessels counted with CD31 staining. Images of collagen I, pimonidazole, α-SMA (cancer associated fibroblast, CAF), TGF-β1, CTGF or VEGF stained sections were analyzed based on the area fraction of positive staining using Image J software. Identical analysis settings and thresholds were used for all tumors.

Colorectal cancer solid stress

Solid stress was measured using the tumor opening technique [3]. The nude mice were anaesthetized on the day of the last treatment. Subsequently, each tumor was excised, washed with Hank's balanced salt solution and its three dimensions were measured. Each tumor was cut along its longest axis, to a depth of 80% of its shortest dimension using a scalpel. The tumors were allowed to relax for 10 min in Hank's balanced salt solution to diminish any transient, poro-elastic responses. Afterwards, the opening resulting from the cut was measured at the middle of the cut at the surface of the tumor. Solid stress is proportional to the size of the opening relative to the size of the dimension perpendicular to the cut.

Colorectal cancer cisplatin delivery and tumor growth

Nude mice bearing ectopic sw620 were split into four groups (6 mice per group) When the tumor volume reached 100 mm^3 post-inoculation, the nude mice were treated with 25.0 $mg \cdot kg^{-1}$ Endostar, 5.0 $mg \cdot kg^{-1}$ cisplatin, combination of 25.0 $mg \cdot kg^{-1}$ Endostar and 5.0 $mg \cdot kg^{-1}$ cisplatin or an equal volume of saline intravenously every other day for 14 days. On the last day of treatment, nude mice were injected with 10.0 $mg \cdot kg^{-1}$ cisplatin, administered retro-orbitally 30 min before tumors and organs removal. The volume and weight of tumors were measured. Then, the tumors and organs were dabbed of excess blood and snap-frozen in liquid nitrogen for analysis. Cisplatin was isolated from the tissues and measured using high performance liquid chromatography (HPLC, Agilent® Technologies, Santa Clara, CA, USA) on a COSMOSIL C18 column (250 mm × 4.5 mm, 5 μm) (Shimadzu, Tokyo, Japan). All responses obtained were analysed using Agilent ChemStation software.

Statistical analysis

All data are presented as the mean ± standard error of the mean of independent triplicate

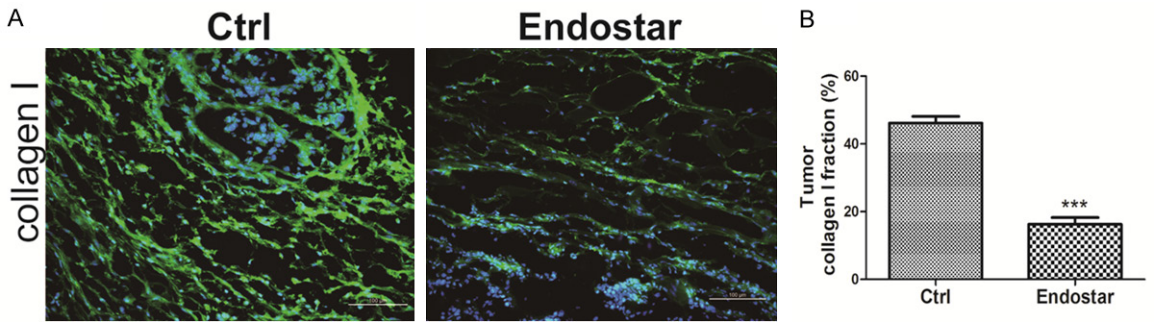

Figure 1. A. Immunofluorescence images showing the effect of Endostar on sw620 tumor stromal collagen I (green) level. Scale bar: 100 μm. B. Quantification of tumor collagen I level following Endostar treatment. Endostar decreases the collagen I positive area fraction in sw620 tumor (n=6, ***P<0.001, Student's t-test). Error bars indicate s.e.m.

samples. The fraction of histology, vascular perfusion and hypoxia were between the control group and the endostar group was conducted by using Student's t-test. The plasma level, tumor solid stress and cisplatin concentration between the two groups also was conducted by using Student's t-test. The tumor weight and volume of the four gourps were performed using one-way ANOVA followed by Bartlett's test for multiple-comparisons. The All statistical analyses were performed using GraphPad Prism (version 5.0; GraphPad Software, La Jolla, CA). *P* values less than 0.05 were considered statistically significant (*P<0.05, **P< 0.01, and ***P<0.001).

Results

Endostar reduces colorectal cancer stromal collagen I

Collagen I plays a vital role in tumor vessel compression, leading to blood flow decline and subsequent tumor areas with no adequate perfusion. In addition, the stiffening as well as organization of the collagen I via CAF have been reported to be involved in tumor cell invasion. In our study, Endostar significantly decreased collagen I expression in tumor (P<0.001, **Figure 1A**, **1B**), possibly through degrading or destabilization of collagen I.

Endostar reduces colorectal cancer stromal fibrosis signalling

To further investigate the tumor stromal fibrosis signaling after Endostar or saline administration, ELISA kit and immunohistochemistry were utilized to evaluate the specific way of Endostar affecting CTGF, VEGF or TGF-β1 expressions in colorectal cancer models. Consequently, Endostar reduced plasma TGF-β1 (P<0.001, **Figure 2A**), CTGF (P<0.001, **Figure 2B**) and VEGF (P<0.001, **Figure 2C**) in nude mice. In addition, the reduction in tumor expression of CTGF, TGF-β1, as well as VEGF by Endostar was verified through immunohistochemistry assess (P< 0.001, **Figure 2D**).

Endostar decreases colorectal cancer CAF density in tumors

In view of the recognized roles of Endostar on collagen I expression, Endostar was then detected for its potential role in decreasing colorectal cancer CAF density. The identification of CAF mostly relies on α-SMA, a typical myocyte marker, as well as other markers, like fibroblast-specific protein (FSP-1). CAFs play an essential part in cancer progression, recurrence as well as metastasis. Here, Endostar diminished the staining density of α-SMA-positive cells in colorectal cancer models (P< 0.001, **Figure 3A**, **3B**), which implied a decreased level of CAF activity. Therefore, Endostar was likely to diminish activation of fibroblasts to α-SMA-positive CAF phenotype.

Endostar lowers solid stress in colorectal cancer

The role of Endostar on solid stress was further explored in colorectal cancer. By employing the recently established techniques, a decline in solid stress after Endostar treatment was detected in colorectal cancer (**P=0.0012, **Figure 4**), implicating the potential role of Endostar, with antimatrix effects, in decompressing

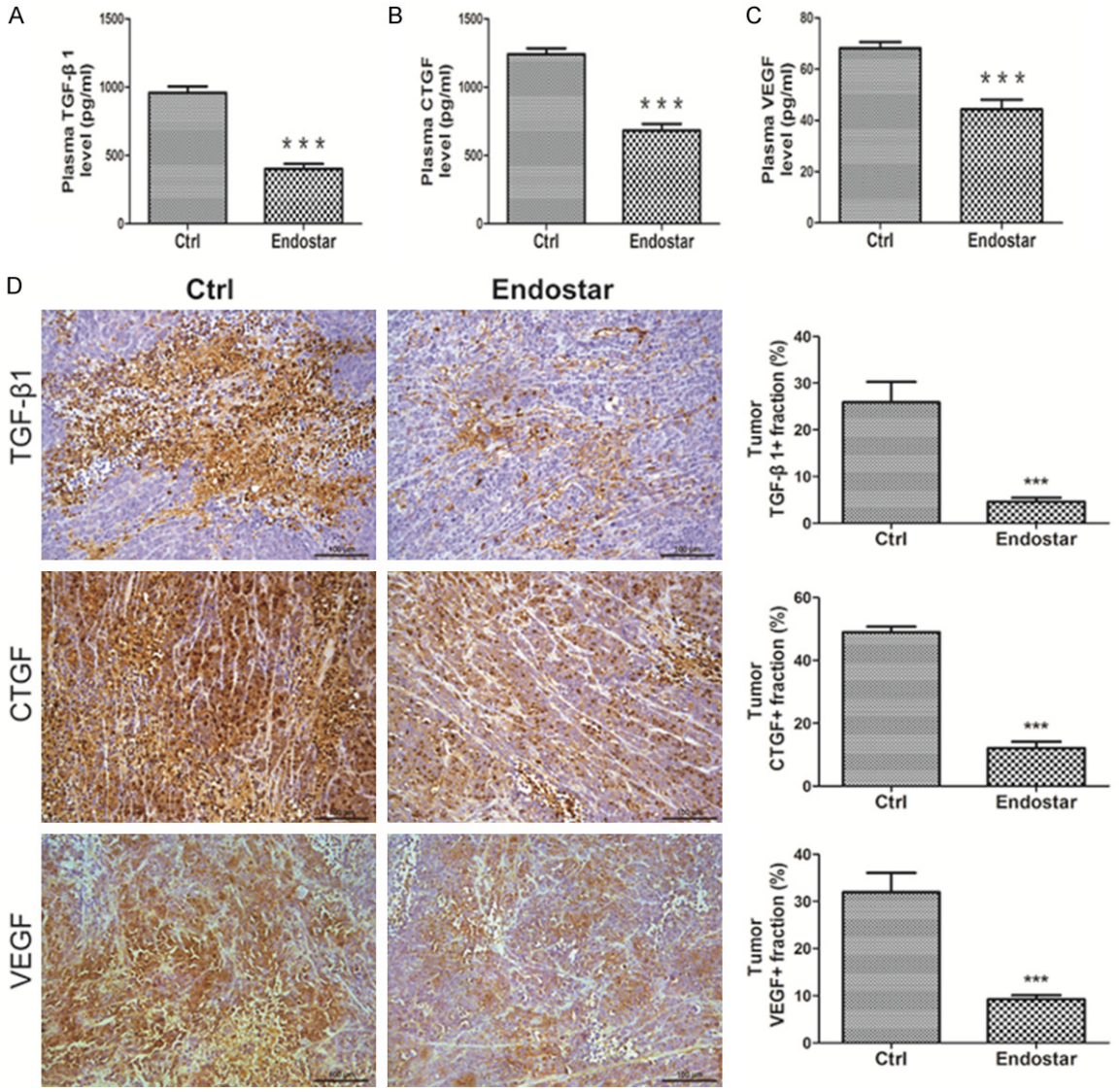

Figure 2. Endostar decreases profibrotic cytokine levels in plasma and sw620 tumor. (A) Plasma level of TGF-β1 was decreased after Endostar treatment (n=6, ***P<0.001, Student's t-test). (B) Plasma level of CTGF was decreased (n=6, ***P<0.001, Student's t-test) and (C) the plasma level of VEGF was decreased after Endostar treatment (n=6, ***P<0.001, Student's t-test). (D) Histology images showing the effect of Endostar on TGF-β1, CTGF and VEGF expression in sw620 tumor (n=6). Scale bar, 100 μm. Endostar reduces the expression of TGF-β1 (***P<0.001, Student's t-test), CTGF (***P<0.001, Student's t-test) and VEGF (***P<0.001, Student's t-test) in sw620 tumor. Error bars indicate s.e.m.

vessels in desmoplastic tumors through solid stress decline.

Endostar increases colorectal cancer vessel perfusion

Next, we assessed whether reduced solid stress by Endostar could enhance vessel perfusion in our desmoplastic tumor models. Consequently, only 11.23% of vessels in the severely hypoperfused tumor of colorectal cancer were initially perfused with blood, which significantly rose to 38.18% after Endostar administration (***P<0.001, **Figure 5A**), indicating that vessel decompression was part of the mechanism. Hence, vessel perfusion in tumors was elevated by Endostar via reducing solid stress.

Endostar enhances oxygen and colorectal cancer cisplatin delivery

In consideration that oxygen as well as drug delivery to tissue was controlled by vessel per-

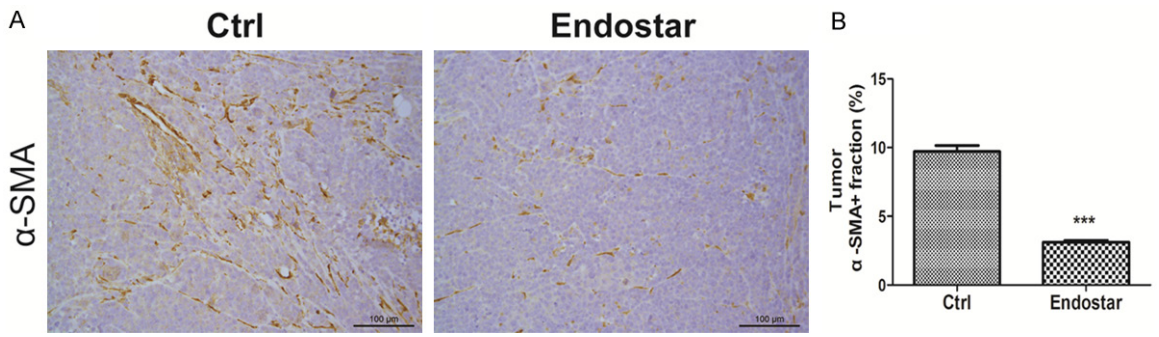

Figure 3. Endostar reduces α-SMA+ CAF density in sw620 tumor. A. Histology images showing the effect of Endostar on tumor α-SMA+ CAF (brown) level. Scale bar, 100 μm. B. Immunohistochemical analysis of α-SMA+ CAF density with Endostar treatment. Endostar reduces the α-SMA+ CAF density in sw620 tumor (n=6, ***P<0.001, Student's t-test). Error bars indicate s.e.m.

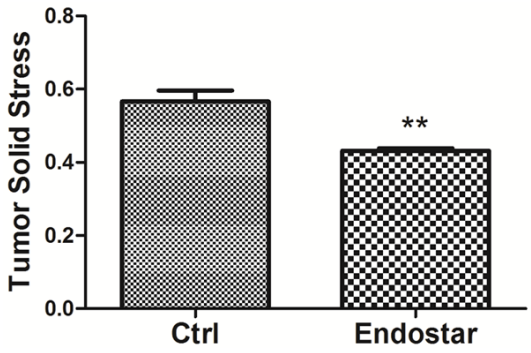

Figure 4. Endostar reduces tumor solid stress in sw620 tumor. Tumor solid stress was assessed using an ex vivo technique involving the measurement of the extent of tumor tissue relaxation (tumor opening relative to tumor diameter) following a stress-releasing incision, with larger openings indicating higher stress. Through its antimatrix effects, Endostar reduces tumor solid stress in sw620 tumor (n=6, **P=0.0012, Student's t-test). Error bars indicate s.e.m.

fusion, the tumor oxygenation was assessed using pimonidazole staining. As a result, Endostar administration sustained tumor oxygen concentrations in SW620 xenograft models, while a typical growth-dependent drop in oxygenation was observed in control group (***P<0.001, **Figure 5B**). Thus, reducing tumor solid stress through 'microenvironmental normalization' with Endostar increases the delivery of oxygen to tumors. Next, we tested the effects of Endostar on drug delivery to tumors. We detected the accumulation of the small-molecule chemotherapeutic cisplatin in tumor, liver and kidney by HPLC. The results showed that Endostar improved cisplatin delivery to sw620 tumor (**P=0.0155, **Figure 5C**) while not affecting delivery to liver (P=0.7931, **Figure 5D**) and kidney (P=0.8515, **Figure 5E**). The data implies that this strategy for enhancing delivery selectively affects tumors, which is expected, since solid stress does not accumulate in most normal organs. Together, these data indicate that treatment with Endostar increases vessel perfusion and alleviates hypoxia in tumors.

Endostar potentiates the efficacy of cisplatin

Based on the above outcomes, we further detected the effects of a combination of Endostar and cisplatin in SW620 xenograft models. Tumor growth was significantly inhibited by both cisplatin monotherapy and cisplatin combined with Endostar (**Figure 6A**, **6B**). As anticipated, a greater inhibition degree of tumor growth was observed in mice undergoing combined therapy than those receiving cisplatin monotherapy. Consistently, HPLC analysis also demonstrated high concentrations of cisplatin from tumors in mice with combined treatment. The above both assays implicated an elevated cisplatin efficacy of Endostar treatment, which was promoted by tumor vessel decompression. Taken together, Endostar was able to increase therapeutic effectiveness of small-molecule agents through its antimatrix effects.

Discussion

In this study, we demonstrate the complicated roles of matrix in blocking drug delivery in tumor tissues. Extracellular matrix (ECM), product of cancer cells, CAFs, as well as other stromal cells, provides structural basis of the tu-

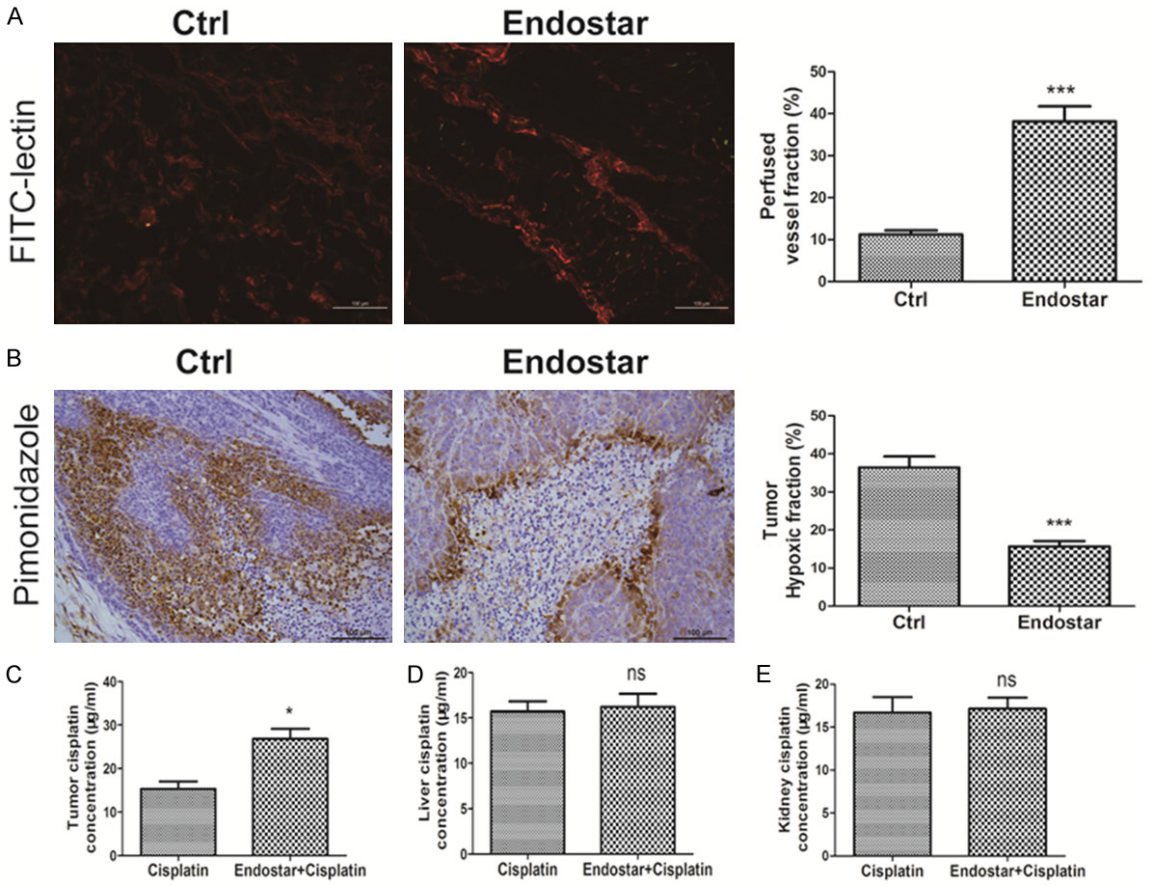

Figure 5. Endostar increases sw620 tumor vascular perfusion and drug delivery, reducing tumor hypoxia. (A) Representative images from immunofluorescence microscopy of perfused tumor vessels (green), showing that Endostar increases the density of perfused vessels in sw620 colorectal cancer (n=6, ***P<0.001, Student's t-test). Scale bar, 100 μm. (B) Hypoxic fraction in tumor measured by pimonidazole injection and staining following Endostar treatment. Endostar reduces the hypoxic fraction in sw620 tumor (n=6, ***P<0.001, Student's t-test) because of the increased oxygen delivery. Scale bar, 100 μm. Cisplatin delivered to the tumor (C), liver (D) and kidney (E) after Endostar treatment. Endostar increases the cisplatin accumulation in sw620 colorectal cancer (n=3, *P=0.0155, Student's t-test), while not affecting cisplatin accumulation in liver (n=3, P=0.7931, Student's t-test) and kidney (n=3, P=0.8515, Student's t-test). Error bars indicate s.e.m.

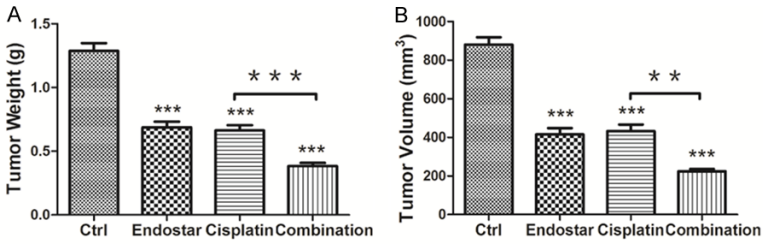

Figure 6. Endostar potentiates the efficacy of cisplatin. A. Volume of ectopic sw620 tumor on day 14 in response to treatment with Endostar, cisplatin, combination of Endostar and cisplatin or saline. B. Weight of ectopic sw620 tumor on day 14 of four treatment group. Cisplatin and Endostar monotherapy induce significant growth delay versus the control treatment, whereas their combination greatly inhibited sw620 tumor growth (n=6, ***P<0.001, One-Way ANOVA). Error bars indicate s.e.m.

mor microenvironment and interacts with cancer cells by molecular communications [15, 16]. Previous studies have reported that fibrosis in liver as well as collagen density in breast are independent risk factors of cancer in these organs [17, 18]. leading to the speculation of the role of fibrosis as well as dense ECM in triggering cancers. In addition, the organization, content as well as the biomechanical natures of ECM aggravate tumor progression. The role of stiffening as well as organization of the collagen fibers by CAF in promoting invasion of cancer cells has been reported in several studies [19, 20].

Despite the limitaions in larger drugs distribution by steric interplays with collagen, the delivery of smaller chemotherapy agents is not directly blocked [21], which, however, is indirectly hindered by vessel compression. The solid stress are enhanced by hyaluronan as well as collagen in tumors. Conversely, low levels of collagen contribute to a more easily expansive tumor microenvironment with vigorous proliferation, subsequently easing compressive stress.

Endostatin, a broad-spectrum endogenous anti-angiogenic agent, plays its role by multiple signaling pathways, including E-selectin, VEGF, bFGF/FGF-2 as well as metalloproteinases [11, 12]. In addition, Endostar, a recombinant agent of Endostatin has been tested in clinical setting of lung cancer therapy [22]. Here, Endostar was found to rapidly decrease established tumor stromal collagen I level, implicating that collagen I was degraded or destabilized by Endostar via an unknown mechanism besides blocking the matrix production through TGF-β1. CTGF is a matricellular protein and plays a role in the stabilization of transient fibrosis induced by TGF-β1 activity [23, 24]. Hence, we speculated that Endostar was able to destabilize collagen I via inhibition of CTGF expression. Endostar reduced both CTGF and TGF-β1 in colorectal cancer models. Thus, Moreover, TGF-β1 as well as CTGF expressions were diminished by Endostar in colorectal cancer models. Taken together, Endostar was able to decrease stromal collagen I production mainly by TGF-β1, plus by destabilization in the existing collagen I through CTGF. VEGF, a homodimeric glycoprotein widely involved in angiogenesis, regulates tumor neovascularization as well as permeability of blood vessels [25, 26]. Recently, the association between VEGF and fibrosis, inflammatory disease has been found. Specifically, increased concentrations of VEGF have been reported in Crohn disease, rheumatoid disease as well as fibrotic ocular disease [27, 28]. Our results showed that Endostar also reduced plasma and tumor VEGF level in nude mice.

CAFs are recognized to be profoundly involved in cancer progression, recurrence as well as metastasis [29]. Here, in our study, Endostar treatment reduced the density of activated CAFs in colorectal cancer models, indicating the potential role of Endostar in decreasing the activation of fibroblasts into α-SMA-positive CAF phenotype, which, in turn, resulted in a decline of CAF density. The above-described effects of Endostar together contribute to reduced collagen I level in colorectal cancer models.

Solid stress mainly originates from fibroblasts stress and is further reserved as strain energy in the ECM, which is later transmitted to compress blood vessels through cooperation between hyaluronan and collagen, ultimately leading to inconsistent, unsatisfactory tissue perfusion as well as hypoxia in the tumor microenvironment [30, 31]. Our results have shown that Endostar reduced solid stress in colorectal cancer, implicating that Endostar, via its anti-matrix effects, is likely to decompress vessels in desmoplastic tumors attributed to reduced solid stress. Moreover, Endostar increased tumor vessel perfusion in the models through the reduction of solid stress. In consideration that oxygen as well as drug delivery to tissue is controlled by vessel perfusion, the tumor oxygenation was assessed using pimonidazole staining. Consequently, Endostar administration sustained tumor oxygen concentrations in SW620 xenograft models, while a typical growth-dependent drop in oxygenation was observed in control group. Hence, reduction of tumor solid stress via 'microenvironmental normalization' mediated by Endostar promoted the oxygen delivery to cancers.

We further determined the cisplatin concentration in tumors using HPLC analysis, which revealed that the concentration of intratumor cisplatin was elevated by Endostar administration, attributed from the blood flow enhancement. These data indicate that only tumor tissues were targeted by the delivery-enhanceing strategy, mainly due to the specific accumulation of solid stress in tumor tissues but not in normal tissues.

In summary, we report for the first time that Endostar enhances vessel perfusion via vascular decompression due to inhibited stromal activity as well as limited matrix components production. Of note, Endostar targets both CAF as well as collagen I, two well-known contributors to solid stress. Moreover, we speculate that inhibitors of downstream signalling through VEGF, TGF-β1 or CTGF can possibly sensitisize chemotherapy by decreasing solid stress. A

clear elucidation on the molecular mechanisms of tumor vessel decompression is necessary in the future. Remarkably, Endostar is a promising agent in cancer therapies for its safety, low cost, as well as the potentiation of conventional chemotherapy.

Conclusion

In this article, we have reported for the first time that Endostar decreased colorectal cancer CAF density, reduced tumor stromal collagen I production, diminished the expression of profibrotic signals, including TGF-β1, CTGF as well as VEGF. Reduced solid stress by Endostar further led to elevated vascular perfusion in tumor. Altogether, oxygen as well as drug delivery to tumors were enhanced, decreasing hypoxic fraction and improving chemotherapeutic effects in colorectal cancer. In spite of the necessity of further studies to explore the mechanisms, Endostar was verified to be a potent therapeutic target by decompressing tumor vascular, and TGF-β1, CTGF or VEGF.

Acknowledgements

This work was supported by the National Natural Science Foundation of China (81472849), the Guangdong Natural Science Research (2014A030313383) and the Guangdong High-level University Construction Fund for Jinan University (88016013034).

Disclosure of conflict of interest

None.

Address correspondence to: Yunlong Pan, Department of General Surgery, The First Affiliated Hospital of Jinan University, Guangzhou 510632, China. Tel: 86-20-38688609; E-mail: tpanyl@jnu.edu.cn

References

[1] Chauhan VP, Stylianopoulos T, Boucher Y and Jain RK. Delivery of molecular and nanoscale medicine to tumors: transport barriers and strategies. Annu Rev Chem Biomol Eng 2011; 2: 281-298.

[2] Jain RK. Normalizing tumor microenvironment to treat cancer: bench to bedside to biomarkers. J Clin Oncol 2013; 31: 2205-2218.

[3] Stylianopoulos T, Martin JD, Chauhan VP, Jain SR, Diop-Frimpong B, Bardeesy N, Smith BL, Ferrone CR, Hornicek FJ, Boucher Y, Munn LL and Jain RK. Causes, consequences, and remedies for growth-induced solid stress in murine and human tumors. Proc Natl Acad Sci U S A 2012; 109: 15101-15108.

[4] Stylianopoulos T, Martin JD, Snuderl M, Mpekris F, Jain SR and Jain RK. Coevolution of solid stress and interstitial fluid pressure in tumors during progression: implications for vascular collapse. Cancer Res 2013; 73: 3833-3841.

[5] Padera TP, Stoll BR, Tooredman JB, Capen D, di Tomaso E and Jain RK. Pathology: cancer cells compress intratumour vessels. Nature 2004; 427: 695.

[6] Janmey PA and McCulloch CA. Cell mechanics: integrating cell responses to mechanical stimuli. Annu Rev Biomed Eng 2007; 9: 1-34.

[7] Park MS, Klotz E, Kim MJ, Song SY, Park SW, Cha SW, Lim JS, Seong J, Chung JB and Kim KW. Perfusion CT: noninvasive surrogate marker for stratification of pancreatic cancer response to concurrent chemo- and radiation therapy. Radiology 2009; 250: 110-117.

[8] Sorensen AG, Emblem KE, Polaskova P, Jennings D, Kim H, Ancukiewicz M, Wang M, Wen PY, Ivy P, Batchelor TT and Jain RK. Increased survival of glioblastoma patients who respond to antiangiogenic therapy with elevated blood perfusion. Cancer Res 2012; 72: 402-407.

[9] Whatcott CJ, Diep CH, Jiang P, Watanabe A, LoBello J, Sima C, Hostetter G, Shepard HM, Von Hoff DD and Han H. Desmoplasia in primary tumors and metastatic lesions of pancreatic cancer. Clin Cancer Res 2015; 21: 3561-3568.

[10] Ohlund D, Elyada E and Tuveson D. Fibroblast heterogeneity in the cancer wound. J Exp Med 2014; 211: 1503-1523.

[11] Folkman J. Antiangiogenesis in cancer therapy--endostatin and its mechanisms of action. Exp Cell Res 2006; 312: 594-607.

[12] O'Reilly MS, Boehm T, Shing Y, Fukai N, Vasios G, Lane WS, Flynn E, Birkhead JR, Olsen BR and Folkman J. Endostatin: an endogenous inhibitor of angiogenesis and tumor growth. Cell 1997; 88: 277-285.

[13] Ling Y, Yang Y, Lu N, You QD, Wang S, Gao Y, Chen Y and Guo QL. Endostar, a novel recombinant human endostatin, exerts antiangiogenic effect via blocking VEGF-induced tyrosine phosphorylation of KDR/Flk-1 of endothelial cells. Biochem Biophys Res Commun 2007; 361: 79-84.

[14] Zhang LP, Liao XY, Xu YM, Yan LJ, Yan GF, Wang XX, Duan YZ and Sun JG. Efficacy and safety of endostar(R) combined with chemotherapy in patients with advanced soft tissue sarcomas. Asian Pac J Cancer Prev 2013; 14: 4255-4259.

[15] Lu P, Weaver VM and Werb Z. The extracellular matrix: a dynamic niche in cancer progression. J Cell Biol 2012; 196: 395-406.

[16] Tung JC, Barnes JM, Desai SR, Sistrunk C, Conklin MW, Schedin P, Eliceiri KW, Keely PJ, Seewaldt VL and Weaver VM. Tumor mechanics and metabolic dysfunction. Free Radic Biol Med 2015; 79: 269-280.
[17] Boyd NF, Guo H, Martin LJ, Sun L, Stone J, Fishell E, Jong RA, Hislop G, Chiarelli A, Minkin S and Yaffe MJ. Mammographic density and the risk and detection of breast cancer. N Engl J Med 2007; 356: 227-236.
[18] Elsharkawy AM and Mann DA. Nuclear factor-kappaB and the hepatic inflammation-fibrosis-cancer axis. Hepatology 2007; 46: 590-597.
[19] Gaggioli C, Hooper S, Hidalgo-Carcedo C, Grosse R, Marshall JF, Harrington K and Sahai E. Fibroblast-led collective invasion of carcinoma cells with differing roles for RhoGTPases in leading and following cells. Nat Cell Biol 2007; 9: 1392-1400.
[20] Goetz JG, Minguet S, Navarro-Lerida I, Lazcano JJ, Samaniego R, Calvo E, Tello M, Osteso-Ibanez T, Pellinen T, Echarri A, Cerezo A, Klein-Szanto AJ, Garcia R, Keely PJ, Sanchez-Mateos P, Cukierman E and Del Pozo MA. Biomechanical remodeling of the microenvironment by stromal caveolin-1 favors tumor invasion and metastasis. Cell 2011; 146: 148-163.
[21] Pluen A, Boucher Y, Ramanujan S, McKee TD, Gohongi T, di Tomaso E, Brown EB, Izumi Y, Campbell RB, Berk DA and Jain RK. Role of tumor-host interactions in interstitial diffusion of macromolecules: cranial vs. subcutaneous tumors. Proc Natl Acad Sci U S A 2001; 98: 4628-4633.
[22] Xiao L, Yang S, Hao J, Yuan X, Luo W, Jiang L, Hu Y, Fu Z, Zhang Y and Zou C. Endostar attenuates melanoma tumor growth via its interruption of b-FGF mediated angiogenesis. Cancer Lett 2015; 359: 148-154.
[23] Mori T, Kawara S, Shinozaki M, Hayashi N, Kakinuma T, Igarashi A, Takigawa M, Nakanishi T and Takehara K. Role and interaction of connective tissue growth factor with transforming growth factor-beta in persistent fibrosis: a mouse fibrosis model. J Cell Physiol 1999; 181: 153-159.
[24] Papageorgis P and Stylianopoulos T. Role of TGFbeta in regulation of the tumor microenvironment and drug delivery (review). Int J Oncol 2015; 46: 933-943.
[25] Siveen KS, Prabhu K, Krishnankutty R, Kuttikrishnan S, Tsakou M, Alali FQ, Dermime S, Mohammad RM and Uddin S. Vascular endothelial growth factor (VEGF) signaling in tumour vascularization: potential and challenges. Curr Vasc Pharmacol 2017; 15: 339-351.
[26] Grothey A. VEGF inhibition beyond tumour progression. Lancet Oncol 2013; 14: 2-3.
[27] Danese S. Inflammation and the mucosal microcirculation in inflammatory bowel disease: the ebb and flow. Curr Opin Gastroenterol 2007; 23: 384-389.
[28] Maruotti N, Cantatore FP, Crivellato E, Vacca A and Ribatti D. Angiogenesis in rheumatoid arthritis. Histol Histopathol 2006; 21: 557-566.
[29] Augsten M. Cancer-associated fibroblasts as another polarized cell type of the tumor microenvironment. Front Oncol 2014; 4: 62.
[30] Zlotek-Zlotkiewicz E, Monnier S, Cappello G, Le Berre M and Piel M. Optical volume and mass measurements show that mammalian cells swell during mitosis. J Cell Biol 2015; 211: 765-774.
[31] Orimo A, Gupta PB, Sgroi DC, Arenzana-Seisdedos F, Delaunay T, Naeem R, Carey VJ, Richardson AL and Weinberg RA. Stromal fibroblasts present in invasive human breast carcinomas promote tumor growth and angiogenesis through elevated SDF-1/CXCL12 secretion. Cell 2005; 121: 335-348.